Two gustatory receptors involved in host plant recognition of silkworm larvae

Haruka Endo[1,2,4,5,*], Kana Tsuneto[2,4], Takayuki Yamagishi[2], Dingze Mang[2,6], Katsuhiko Ito[3], Shinji Nagata[1] and Ryoichi Sato[2,*]

[1]Department of Integrated Bioscience, Graduate School of Frontier Sciences, The University of Tokyo, Kashiwa, Chiba 277-8562, Japan

[2]Graduate School of Bio-Applications and Systems Engineering, Tokyo University of Agriculture and Technology, Koganei, Tokyo 184-8588, Japan

[3]Department of Science of Biological Production, Graduate School of Agriculture, Tokyo University of Agriculture and Technology, Fuchu,Tokyo 183-8509, Japan

[4]The authors contributed equally.

[5]Present address: RIKEN Center for Brain Science, 2-1 Hirosawa, Wako, Saitama 351-0198, Japan

[6]Present address: College of Life Science, Institute of Life Science and Green Development, Hebei University, Baoding 071002, China

*Correspondence: haruka.endo@riken.jp (H.E.) or ryoichi@cc.tuat.ac.jp (R.S.).

Abstract

Herbivorous insects can identify their host plants by sensing plant secondary metabolites as chemical cues. We previously reported the two-factor host acceptance system of the silkworm *Bombyx mori* larvae. The chemosensory neurons in the maxillary palp (MP) of the larvae detect mulberry secondary metabolites, chlorogenic acid (CGA), and isoquercitrin (ISQ), with ultrahigh sensitivity, for host plant recognition and feeding initiation. Nevertheless, the molecular basis for the ultrasensitive sensing of these compounds remains unknown. In this study, we demonstrated that two gustatory receptors (Grs), BmGr6 and BmGr9, are responsible for sensing the mulberry compounds with attomolar sensitivity for host plant recognition by silkworm larvae. Calcium imaging assay using cultured cells expressing the silkworm putative sugar receptors (BmGr4-10) revealed that BmGr6 and BmGr9 serve as receptors for CGA and ISQ with attomolar sensitivity in human embryonic kidney 293T cells. CRISPR/Cas9-mediated knockout (KO) of BmGr6 and BmGr9 resulted in a low probability of making a test bite of the mulberry leaves, suggesting that they lost the ability to recognize host leaves specifically. Electrophysiological recordings showed that the loss of host recognition ability in the Gr-KO strains was due to a drastic decrease in MP sensitivity toward ISQ in BmGr6-KO larvae and toward CGA and ISQ in BmGr9-KO larvae. Our findings unraveled that the two Grs, which have been regarded as sugar receptors, are molecules responsible for detecting plant phenolics in host plant recognition.

Keywords: herbivorous insects, host plant selection, plant secondary metabolites; silkworm; gustatory receptors

Introduction

Many herbivorous insects have specialized on a limited range of plants as their hosts through ecological and evolutionary interactions with plants. Plants have various physical and chemical defense mechanisms to combat insect herbivory (War et al., 2012). For instance, plants have evolved a variety of secondary metabolites, most of which act as feeding deterrents and are often toxic to herbivorous insects (Fraenkel, 1959). In turn, herbivorous insects have adapted to some of the chemicals by developing chemosensory systems, enzymatic detoxication, and other mechanisms, which enabled them to consume a specific limited range of plants (Heidel-Fischer and Vogel, 2015; Simon et al., 2015). In parallel, they were able to identify host plants using plant secondary metabolites as sensory cues (Chapman, 2003).

Sensory exploration at the leaf surface is essential for host plant selection in larval feeding and adult ovipositioning (Chapman and Bernays, 1989; Renwick, 1989). We previously reported that the silkworm *Bombyx mori* larvae, well known for their preference for mulberry leaves, feed on the leaves utilizing a two-factor authentication system controlled by two taste organs and a set of chemoreceptors with differing sensitivities, operating sequentially in time (Tsuneto et al., 2020). The first step involves probing the leaf surface with the maxillary palp (MP), which contains ultrasensitive chemosensory neurons sensitive to a set of crucial mulberry compounds, including secondary metabolites (chlorogenic acid [CGA] and quercetin glycosides) and a phytosterol (β-sitosterol). The ultrahigh sensitivities in the attomolar and femtomolar ranges enable the larvae to detect trace amounts of these compounds at the dry leaf surface (Chapman and Bernays, 1989; Cheng et al., 2017) and identify the host leaves. If these three compounds are detected simultaneously, the larva makes a test bite, which leads to the second step. Another gustatory organ, the maxillary galea (MG), is used to probe the sugar content released by the test bite. Sucrose mainly induces continued biting, resulting in feeding. The two-factor host acceptance system is expected to be conserved among herbivorous insects because of their typical stepwise feeding behavior, composed of foraging, palpation at the leaf edge, test and persistent biting, and swallowing (Chun, 1972; Devitt and Smith, 1985). Although understanding the behavioral and neural basis of host acceptance in silkworm larvae has progressed, the molecular basis underlying MP's ultrasensitive detection of the mulberry compounds remains unknown.

While, to our knowledge, no previous studies have identified lepidopteran chemosensory receptors responsible for host plant selection in larval feeding, two examples have been reported in adult oviposition. A gustatory receptor (Gr) PxutGr1 from the swallowtail butterfly *Papilio xuthus* is responsible for the sensitivity of tarsal taste sensilla to synephrine and the oviposition behavior induced by a mixture of synephrine and *chiro*-inositol (Ozaki et al., 2011). The two olfactory receptors (Ors) in *Plutella xylostella*, Or35 and Or49, are necessary and sufficient for detecting isothiocyanates

76 and isothiocyanates-mediated oviposition preference for its host cruciferous plants (Liu et al., 2020).
77 Meanwhile, some Grs have been reported as receptors for plant secondary metabolites in
78 lepidopteran insects, although the importance in the ecology of the insect species is unclear.
79 PrapGr28 from the cabbage butterfly, *Pieris rapae*, contributes to sinigrin sensitivity in adult tarsal
80 taste sensilla (Yang et al., 2021), although sinigrin is a feeding stimulant for their larvae (Renwick and
81 Lopez, 1999). PxylGr34 from the diamondback moth, *Plutella xylostella*, is involved in response to
82 canonical plant hormones, brassinolide, and 24-epibrassinolide, a feeding and oviposition deterrent,
83 in MG of larvae (Yang et al., 2020). In addition, BmGr16, BmGr18, and BmGr53 from *B. mori* respond
84 to coumarin and caffeine in human embryonic kidney 293T (HEK293T) cells (Kasubuchi et al., 2018),
85 but their role *in vivo* is unknown. Thus, several examples of relatively low-sensitive chemoreceptors
86 for plant secondary metabolites in the foreleg of adult and MG of larvae have been reported. However,
87 ultrahigh-sensitive chemoreceptors in larval MP underlying the first step in the two-factor host
88 acceptance system are unknown.
89 We addressed the molecular basis of host recognition in silkworm larvae in the present study. *In vitro*
90 calcium imaging in the cells suggested that BmGr6 and BmGr9 are candidates that confer MP
91 ultrahigh sensitivity for CGA and ISQ. CRISPR/Cas9-mediated KOs demonstrate that the two Grs are
92 responsible for host recognition by sensing CGA and/or ISQ.
93
94 **Results**
95 **BmGr6 and BmGr9 serve as ultrahigh-sensitive receptors for CGA and ISQ as well as sugar**
96 **receptors in HEK293T cells**
97 We started with phylogenetic analysis to find closely related silkworm Grs with PxutGr1 as candidate
98 receptors for CGA and ISQ because PxutGr1 is the only lepidopteran Gr reported as a receptor for
99 plant phenolics (Ozaki et al., 2011). Phylogenetic analysis of lepidopteran Grs indicates that PxutGr1
100 belongs to the same lineage as BmGr9 and BmGr10, known as fructose and *myo*-inositol receptors,
101 respectively (Kikuta et al., 2016; Sato et al., 2011) (Fig. 1). Based on the phylogenetic analysis, we
102 focused on BmGr9, BmGr10, and other five Grs (BmGr4-8) in the neighboring putative sugar receptor
103 clade (Wanner and Robertson, 2008).
104 To test whether these seven Grs can confer silkworm MP chemosensory neurons attomolar sensitivity
105 to CGA and ISQ, we performed calcium imaging in HEK293T cells. Of the seven Grs-expressing cells,
106 BmGr6-, BmGr8-, and BmGr9-expressing cells responded to 100 aM CGA, and BmGr6- and BmGr9-
107 expressing cells responded to 100 aM ISQ (Fig. 2A-C). We recorded a dose-dependent response of
108 BmGr6, BmGr8, BmGr9, and BmGr10 (Fig. 2D and E) and determined the EC_{50} values (Table S1).
109 Although BmGr6- and BmGr9-expressing cells responded to <10 aM CGA and ISQ, BmGr8-
110 expressing cells did not respond to 10 aM CGA (Fig. 2D). Based on these results, we focused on and
111 further characterized BmGr6 and BmGr9 as candidates conferring MP neurons attomolar sensitivities
112 toward CGA and ISQ. BmGr6- and BmGr9-expressing cells did not respond to β-sitosterol up to 2 μM
113 (Fig. S1).

114 Since BmGr6 is regarded as a putative sugar receptor (Wanner and Robertson, 2008) and BmGr9
115 was reported as a fructose receptor (Sato et al., 2011), we investigated their response to major sugars
116 present in the mulberry leaves (D-fructose, D-glucose, sucrose, and *myo*-inositol) (Kikuta et al., 2016).
117 Surprisingly, BmGr9-expressing cells responded to D-fructose with aM sensitivity (Fig. 2C and D),
118 whereas they exhibited relatively lower sensitivities to D-glucose, sucrose, and *myo*-inositol (Fig. 2E
119 and F). BmGr6-expressing cells showed pM to nM sensitivity to four sugars (Fig. 2C-F). These results
120 indicate that the two Grs are highly tuned to CGA and ISQ, whereas BmGr9 also exhibits a high
121 affinity with D-fructose.
122
123 **BmGr6 and BmGr9 are expressed in subsets of MP chemosensory neurons**
124 According to the RNA-seq data from a previous study, BmGr6 and BmGr9 are highly expressed in
125 the MP (Guo et al., 2017). To confirm this at the protein level, we performed immunohistochemistry
126 using anti-BmGr6 and anti-BmGr9 antisera. Each sensillum in MP contains three to five
127 chemosensory neurons whose somas are usually clustered in the second segment (Fig. 3A and 3B)
128 (Asaoka, 2003). We observed three BmGr6-antiserum-positive MP neurons (Fig. 3C). In the two
129 representative cryosections, two of the three neurons are close to each other (Fig. 3C), suggesting
130 that the two neurons are contained in the same sensillum. We observed seven BmGr9-antiserum-
131 positive MP neurons, three of which are close to each other (Fig. 3D). Thus, BmGr6 and BmGr9 are
132 expressed in at least three and seven neurons in the MP of silkworm larvae.
133
134 **BmGr6-KO and BmGr9-KO larvae lose their ability to recognize mulberry leaves specifically**
135 To test whether the two Grs are involved in host recognition *in vivo*, we generated BmGr6-KO and
136 BmGr9-KO silkworm strains via the CRISPR/Cas9 system. We designed single-guide RNAs
137 (sgRNAs) targeting the exons 5 and 3 of the *BmGr6* and *BmGr9* genes (Fig. 4A). By injecting the
138 sgRNAs and the Cas9 protein into eggs, we successfully established mutant strains carrying
139 homozygous null mutations of *BmGr6* and *BmGr9* (material and methods for details). In both strains,
140 premature stop codons were generated via indel mutations (Fig. 4A and S2).
141 The body mass of the fifth instar larvae of BmGr6-KO and BmGr9-KO strains, which have been fed
142 with artificial diets since hatching, were ~86% and ~91% of the body mass of wild-type (WT) larvae
143 (Fig. 4B). Since BmGr6 and BmGr9 are expressed in neurosecretory cells in the brain,
144 enteroendocrine cells in the midgut, and other cells in a diversity of organs (Mang et al., 2016; D.
145 Mang et al., 2016), many factors could influence the body mass in the mutant lines in addition to
146 gustation. To directly see the effects of Gr knockouts on feeding, we conducted 1.5 h short-term
147 feeding assay using artificial diets and mulberry leaves. When feeding on leaves, the larvae must
148 recognize host leaves by MP to initiate feeding (the first step of the host acceptance system) (Tsuneto
149 et al., 2020). This step can be skipped when feeding artificial diets with abundant sugars on their
150 surface are available. The feeding amount of artificial diets by BmGr6-KO larvae was ~85% of the WT
151 larvae (Fig. 4C), suggesting that the low body mass of BmGr6-KO larvae is due to the low feeding

152 amount of artificial diets. The feeding amount of BmGr9-KO larvae is comparable with that of WT (Fig.
153 4C). Metabolic factors and factors that affect long-term feeding, such as the interval of feeding, might
154 cause the low body mass of BmGr9-KO larvae. The feeding amounts of mulberry leaves by the two
155 mutant larvae were significantly lower than the WT (Fig. 4D). To directly observe the ability of host
156 recognition, we next observed test bites toward mulberry leaves. Only 33% and 35% of BmGr6-KO
157 and BmGr9-KO larvae made test bites within 1 min, whereas 90% of WT larvae made test bites (Fig.
158 4E). This low probability of test biting corresponds to those of some nonhost leaves in WT larvae
159 (Tsuneto et al., 2020), suggesting that the two mutant strains lose their ability to recognize mulberry
160 leaves. Even when BmGr6-KO and BmGr9-KO larvae were making test bites within 1 min, and their
161 palpation time until making a first test bite was significantly longer than that of WT larvae (Fig. 4F),
162 suggesting that even if mutant larvae made a test bite, they were not able to recognize mulberry
163 leaves immediately. These results indicate that BmGr6 and BmGr9 are essential for host recognition
164 *in vivo*.
165
166 **BmGr6 and BmGr9 are responsible for sensing ISQ and both CGA and ISQ, respectively: *in***
167 ***vivo***
168 We performed electrophysiological recordings from MP to test whether the two Grs are involved in
169 CGA and ISQ sensing *in vivo*. The MP neurons of BmGr6-KO larvae started responding to CGA from
170 10 aM and showed almost the same sensitivity as WT larvae (Fig. 5A and B); they did not respond to
171 ISQ up to 1 μM (Fig. 5A and C). This suggests that the ISQ sensitivity of BmGr6-KO larvae was >10^{10}-
172 fold lower than the MP neurons of WT larvae. By contrast, both CGA and ISQ sensitivities of BmGr9-
173 KO larvae were ~1,000-fold lower than those of WT larvae (Fig. 5A-C), suggesting that BmGr9 is
174 required for attomolar sensitivities of both CGA and ISQ. We previously reported that the β-sitosterol
175 sensitivity of MP neurons is at the femtomolar level (Tsuneto et al., 2020). The number of spikes
176 toward 10 fM β-sitosterol was comparable between WT, BmGr6-KO, and BmGr9-KO strains (Fig. S3),
177 suggesting that MP of the two mutant strains preserved the sensitivity to β-sitosterol. Note that
178 although spikes with multiple shapes derived from different MP chemosensory neurons were
179 expected, we did not observe such spikes but rather observed spikes that are similar to those of single
180 neurons. This may be due to whole MP sensilla recording. Single MP sensillum recording and other
181 imaging methods should be established to clarify how many chemosensory neurons respond. Taken
182 together, BmGr6 and BmGr9 are required for the attomolar sensitivity to ISQ, and BmGr9 is required
183 for attomolar sensitivity to CGA; nevertheless, BmGr6 is not involved in CGA sensing *in vivo*. Unlike
184 *in vitro* study observations in Fig. 2, these results indicate different roles of BmGr6 and BmGr9 *in vivo*.
185
186 **Discussion**
187 **Functional unit of Grs: molecular basis of CGA and ISQ sensing**
188 Ligand identification of insect Grs using heterologous expression systems (e.g., human cultural cells
189 and *Xenopus* oocytes) has often been unsuccessful and yielded little information. In the present study,

190 we identified some ligands of silkworm Grs. The EC_{50} value of BmGr9 to D-fructose from the present
191 study (aM level) is significantly lower than that previously reported by Sato *et al*. (mM level) (Sato et
192 al., 2011). They did not observe BmGr9 response to D-glucose, sucrose, and *myo*-inositol up to 100
193 mM using calcium imaging assay in the HEK293T cells (Sato et al., 2011). It is possible that
194 differences in Gr expression levels and calcium indicators may be responsible for the differences in
195 susceptibility, but further investigation is needed to fully understand the cause of this discrepancy.
196 Meanwhile, the CRISPR/Cas9-mediated KOs of BmGr6 and BmGr9 demonstrated that they could
197 confer the MP attomolar sensitivity to the mulberry compounds (Fig. 5) in partial agreement with the
198 results from calcium imaging using HEK293T cells (Fig. 2).
199 Our results confirm that single Gr can fully function as a receptor *in vitro*; nevertheless, it is evident
200 that heterologous expression of single Gr does not fully reconstitute its function *in vivo*. For example,
201 although BmGr6 served as a CGA receptor with attomolar sensitivity in HEK-293T cells (Fig. 2), the
202 KO of BmGr6 did not influence the MP sensitivity of CGA (Fig. 5). This is not due to functional
203 redundancy with other Grs, as the KO of BmGr9 resulted in a drastic decrease in CGA sensitivity (Fig.
204 5). It is possible that BmGr6 in MP neurons does not function as a homomeric complex but function
205 as a heteromeric complex by coupling with other Grs, as proposed in Ors in general and in some Grs
206 (Del Mármol et al., 2021; Jiao et al., 2008; Shim et al., 2015; Vosshall et al., 1999), resulting in different
207 ligand spectra and sensitivity from the homomeric complex. Otherwise, the difference in the
208 expression levels and other factors between HEK293T cells and MP neurons may affect the
209 contribution of BmGr6 to the CGA sensitivity in MP neurons. Another example is that both BmGr6 and
210 BmGr9 are indispensable for ISQ sensing with attomolar sensitivity (Fig. 5), suggesting a synergism
211 between BmGr6 and BmGr9 to realize the attomolar sensitivity. In this case, too, one possibility is
212 that the two Grs couples in a functional heteromeric complex. Altogether, our results suggest that
213 BmGr6 and BmGr9 function as a heteromeric complex in MP neurons. Although the heterologous
214 expression of single Grs significantly contributed to the screening for Grs with attomolar sensitivity to
215 CGA and ISQ, its utility for dissecting *in vivo* molecular gustatory systems is limited. We cannot rule
216 out the possibility that Grs with lower sensitivities to CGA and ISQ than BmGr6 and BmGr9 and even
217 those with no sensitivities *in vitro* are involved in attomolar sensing in MP by synergism with the two
218 Grs. To understand insect gustatory systems, it is required to decipher functional combinations of Grs
219 and the mechanism determining their ligand spectra.
220
221 **Putative fructose and sugar Grs in the silkworm act as plant phenolics receptors**
222 We demonstrate that BmGr6 and BmGr9 are responsible for ultrahigh-sensitive detection of CGA
223 and/or ISQ. The clades to which BmGr6 and BmGr9 belong are known as sugar receptor clades
224 (Wanner and Robertson, 2008). Nevertheless, we found that they are highly tuned to CGA and ISQ
225 *in vitro* and responded to sugars at relatively high concentrations (Fig. 2). As there was no drastic
226 decrease in the feeding amount of the artificial diet in BmGr6-KO and BmGr9-KO larvae in comparison
227 with the WT (Fig. 4C), it is unlikely that BmGr6 and BmGr9 also act as sucrose receptors in the MG.

228 Unfortunately, we could not provide direct evidence for that because we failed to record spikes from
229 sugar-sensing neurons in the MG of the N4 silkworm strains (both WT and mutants), probably
230 because of their small amplitudes. Our data suggest that the two Grs act as plant phenolics receptors
231 rather than sugar receptors in silkworm larvae's gustatory system. Phenolics are the most widely
232 distributed plant secondary metabolites and serve as stimulants and deterrents toward insects in
233 feeding and oviposition (Singh et al., 2021). Some Grs in the putative sugar and fructose receptor
234 clades may be receptors for plant phenolics which are responsible for host plant selection in
235 herbivorous insects.
236

237 **The attomolar sensitivity is required for sensing leaf surface compounds in host plant**
238 **selection**

239 The experiments using BmGr6-KO and BmGr9-KO larvae provided further insights into the host
240 recognition by MP. BmGr6-KO larvae lost their ability to sense ISQ but could still detect the remaining
241 two test bite inducers (CGA and β-sitosterol) with the same ultrahigh sensitivity as the WT larvae (Fig.
242 5 and S3). Their low probability of test biting toward mulberry leaves (Fig. 4) confirmed the obligate
243 authentication of the three compounds by MP. BmGr9-KO larvae have ~1,000-fold lower sensitivity
244 toward CGA and ISQ. However, they exhibited high sensitivity even at the femtomolar level (Fig. 5),
245 resulting in a lack of host recognition ability with high probability (Fig. 4E). This indicates that the
246 femtomolar sensitivity is insufficient, and the attomolar sensitivity is required to sense leaf surface
247 secondary compounds for host recognition. We recently showed silkworm MP's attomolar sensitivity
248 toward feeding deterrents, such as coumarin and strychnine nitrate (Shii et al., 2021). These ultrahigh
249 sensitivities underlie feeding decisions by herbivorous larvae at the leaf surface.
250 In summary, we identified the two silkworms Grs responsible for the ultrahigh sensitivity in MP to
251 sense leaf surface host phenolic compounds and recognize host leaves. Mechanistic insight into the
252 gustatory system in herbivorous insects, especially on a functional unit of Grs, is needed to know how
253 their Grs have adapted their tunings to plant secondary metabolites and their contribution to the
254 evolution of feeding preferences.

255 **Material and methods**

256 **Chemicals**

chemicals	source	identifer	CAS RN
chrologenic acid	Nacalai tesque	08416-14	327-97-9
isoquercetrin	Extrasynthese	1327S	482-35-9
β-sitosterol	Abcam	ab143122	83-46-5
D-glucose	Fujifilm Wako Pure Chemical Corp.	049-31165	50-99-7
D-fructose	Fujifilm Wako Pure Chemical Corp.	127-02765	57-48-7
sucrose	Fujifilm Wako Pure Chemical Corp.	196-00015	57-50-1
myo-inositol	Fujifilm Wako Pure Chemical Corp.	092-00282	87-89-8

257

258 **Insect rearing**
259 The silkworm *Bombyx mori* larvae (N4 strain and Kinshu × Showa hybrid) were reared at 25°C on an
260 artificial diet Silkmate 2M (Nihon-Nosan Co. Ltd.) under a 12 h light–12 h dark photoperiod. The N4
261 larvae were used for experiments in Fig. 2, 4, 5, S3, and S4. The Kinshu × Showa larvae were used
262 for immunostaining in Fig. 3.
263
264 **Phylogenetic analysis**
265 The lepidopteran Gr phylogeny was generated using full-length amino acid sequences of Grs from
266 *Bombyx mori* (Guo et al., 2017), *P. xylostella* (Engsontia et al., 2014), *H. melpomene* (Briscoe et al.,
267 2013), PxutGr1 (Ozaki et al., 2011), and PrapGr28 (Yang et al., 2021). The sequences were aligned
268 with MAFFT v.7 (http://mafft.cbrc.jp/alignment/server/). The IQ-TREE web server
269 (http://iqtree.cibiv.univie.ac.at/) generated the maximum-likelihood tree using the JTT+F+I+G4 model.
270 The phylogenetic tree was visualized using iTOL (https://itol.embl.de/) (Letunic and Bork, 2021).
271
272 **cDNA cloning of *Bombyx* Grs**
273 cDNA of BmGr6, BmGr7, BmGr9, and BmGr10 were cloned into the pcDNA3.1 vector (Thermo Fisher
274 Scientific) as reported previously (Kikuta et al., 2016; D. Mang et al., 2016). According to the
275 nucleotide sequences reported by Guo *et al*. (Guo et al., 2017), cDNA of BmGr4, BmGr5, and BmGr8
276 were codon-optimized for mammalian cell expression, artificially synthesized (gBlocks®, Integrated
277 DNA Technologies), and inserted into the EcoRV site of pcDNA3.1 vector using GeneArt® Seamless
278 Cloning and Assembly Enzyme Mix (Thermo Fisher Scientific).
279
280 **Cell culture and transfection**
281 HEK293T cells were cultured in Dulbecco's modified Eagle medium (DMEM, Thermo fisher scientific)
282 supplemented with 10% fetal bovine serum (BioWest), 4 mM GlutaMAX (Thermo Fisher Scientific),
283 100 units/ml penicillin (Meiji Seika Pharma Co., Ltd.), and 100 mg/ml streptomycin (Meiji Seika
284 Pharma Co., Ltd.) with 5% CO_2 at 37°C. For preparing transfection solutions, 500 μL Opti-MEM
285 (Thermo Fisher Scientific) were vortexed with 4–6 μg polyethylenimine (PEI Max, Polysciences, Inc.,
286 Warrington, PA) and incubated for 5 min. Afterward, 2 μg of an expression vector was added, vortexed
287 vigorously, and incubated for 20 min. Approximately 50%–70% confluent HEK293T cells were seeded
288 on a coverslip in a six-well plate and transfected with the transfection solution for 4 h with 5% CO_2 at
289 37°C. The media was replaced with DMEM, and the cells were incubated for 48 h.
290
291 **Calcium imaging**
292 For preparing the loading solution of Ca^{2+} indicator Fluo-4 AM (Thermo Fisher Scientific), 3 μL of
293 1 mM Fluo-4 AM (stock solution in DMSO) and 30 μL of PowerLoad Concentrate (100X, Thermo
294 Fisher Scientific) were vortexed vigorously. The mixture (5 μL) was added into a six-well plate
295 containing 500 μL Hank's buffered saline solution (HBSS, 137 mM NaCl, 5.4 mM KCl, 0.3 mM

296 Na_2HPO_4, 0.4 mM KH_2PO_4, 4.2 mM $NaHCO_3$, 1.3 mM $CaCl_2$, 0.5 mM $MgCl_2$, and 0.4 mM $MgSO_4$, pH
297 7.4) incubated for 10 min at 37°C (final conc. ~1 μM Fluo4-AM and ~1X PowerLoad). After loading,
298 the solution was replaced with HBSS containing 0.75 mM Probenecid (Thermo Fisher Scientific). After
299 1 h incubation, the cells were used for calcium imaging experiments.
300 Calcium imaging was performed with a flow system under the fluorescence microscope BX53
301 (Olympus) equipped with a MetaView imaging system (Molecular Devices). A coverslip on which
302 transfected cells were seeded was inverted and put on a self-manufactured chamber with a 5-mm-
303 wide flow channel. The HBSS buffer was superfused at a proper flow rate in a silicon tube with
304 peristaltic pumps (PERISTA pump, ATTO). 200 μL of ligand solution was loaded into the tube with
305 small bubbles back and forth to separate it from HBSS. CGA (Nacalai tesque, Kyoto, Japan), ISQ
306 (Extrasynthese, Lyon, France), D-glucose, D-fructose, sucrose, and *myo*-inositol (Fujifilm Wako Pure
307 Chemical Corp., Osaka, Japan) were dissolved and serially-diluted in HBSS at time of use. β-sitosterol
308 (Abcam, Cambridge, UK) was dissolved in a 45% solution of 2-hydroxypropyl-β-cyclodextrin at 37°C
309 to prepare stable aqueous solutions. The time-lapsed fluorescence images (1 Hz) were processed
310 using Fiji (Schindelin et al., 2012), and the fluorescent ratio (ΔF/F) was calculated as peak intensity
311 divided by basal intensity (mean of 10 flames before ligand perfusion). The EC_{50} value was calculated
312 by fitting using the four-parameter logistic model (Prism ver.8, Graph-Pad).
313
314 **Immunostaining**
315 The heads of the fifth instar larvae (Kinshu × Showa hybrid) were fixed with 4%
316 paraformaldehyde/phosphate-buffered saline (PBS, 137 mM NaCl, 2.7 mM KCl, 10 mM Na_2HPO_4,
317 1.8 mM KH_2PO_4, pH 7.4) overnight at 4°C. The fixed heads were dissected, and the maxilla was
318 collected and immersed into a cryoprotection solution (10% sucrose/PBS at room temperature (RT)
319 for 3 h; 20% sucrose/PBS at 4°C overnight; 30% sucrose/PBS at 4°C overnight), embedded in Tissue-
320 Tek O.C.T. Compound (Sakura Finetek Japan Co., Ltd) and stored at −80°C. The embedded
321 specimens were sectioned at 14 μm thickness via cryostat (CM3050S, Leica, Wetzlar, Germany),
322 mounted on the coated slide glasses (MAS-03, Matsunami Glass, Osaka, Japan), and air dried at RT
323 for a day. After 5 min washes with Tris-NaCl-Tween buffer (TNT; 0.15 M Tris-HCl, 0.01 M NaCl, 0.05%
324 Tween20), the sections were permeabilized with 0.1% TritonX-100/TNT for 5–10 min, blocked with
325 2% bovine serum albumin (BSA)/TNT for 30 min, and incubated with primary antiserum raised
326 elsewhere (Mang et al., 2016; D. Mang et al., 2016) (anti-BmGr6 and anti-BmGr9 antisera in 2%
327 BSA/TNT at a 1:100 dilution) for 12 h at 4°C. The specificities of these antisera were confirmed by
328 testing cross-reactivity of closely related BmGr proteins (Mang et al., 2016; D. Mang et al., 2016).
329 After three 5 min washes with TNT, the sections were incubated in a secondary antiserum (an
330 antimouse IgG conjugated with Alexa Fluor 488, Molecular Probes, USA), at a 1:1,000 dilution in TNT
331 for 12 h at 4°C. After three TNT washes for 5 min, the sections were counterstained with 4, 6-
332 diamidino-2-phenylindole (l mg/mL, Sigma Aldrich, Schnelldorf, Germany) for 5 min at RT. After 5 min

333 of TNT wash, the sections were mounted in 90% glycerol/PBS containing 1, 4-diazabicyclo[2.2.2]
334 octane at RT and observed under fluorescence microscopy (BX53, Olympus, Tokyo, Japan).
335
336 **Generation of Gr-KO silkworm strains using CRISPR/Cas9 genome editing**
337 We used the Alt-R® CRISPR-Cas9 system (Integrated DNA Technologies) to generate silkworm
338 strains carrying null mutations in *BmGr6* or *BmGr9* genes. CRISPRdirect (Naito et al., 2015) identified
339 unique target sequences for guide RNAs using *Bombyx mori* genome assembly as a reference. The
340 off-target search against silkworm genomic sequence confirmed that the designed sgRNAs were
341 highly specific to the target sequences and had only one match (no predicted off-target sites) in
342 20mer+PAM and 12mer+PAM search. Therefore, we consider that do not cause off-target effects
343 theoretically. Alt-R® crRNAs (for BmGr6: 5′-GTATTCGGCGGCGCTGGGAATGG-3′; for BmGr9, 5′-
344 CTGGTGGCGGAGATAGGAGTGGG-3′), tracrRNA, and S.p. Cas9 Nuclease V3 were purchased
345 from Integrated DNA Technologies. CRISPR-Cas9 ribonucleoprotein (RNP) complexes containing 10
346 μM crRNA:tracrRNA duplex and 300 ng/μL Cas9 enzyme were prepared according to a user-
347 submitted protocol entitled "CRISPR-Cas9 RNP delivery—*B. tryoni* microinjection—A Choo" on the
348 Integrated DNA Technologies website. Newly laid eggs of the WT N4 strain were aligned and glued
349 onto a sliding glass, and RNP complexes were injected using IM 300 Microinjector (NARISHIGE)
350 within 5–8 h after oviposition. Generation 0 (G_0) moths were crossed with WT moths. To identify
351 Generation 1 (G_1) broods carrying a heterozygous Cas9-induced mutation, genomic DNA extracted
352 from ~10 G_1 eggs were used for the T7 Endonuclease I (T7EI) assay with Alt-R® Genome Editing
353 Detection Kit (Integrated DNA Technologies). T7EI assay-positive G_1 moths were subjected to sibling
354 mating or crossed with WT moths. Mutations were identified by DNA sequencing of genomic PCR
355 (gPCR) products. Mutant strains carrying a homozygous null mutation were generated by
356 intercrossing G_2 or G_3 moths.
357
358 **Feeding behavior assays**
359 The feeding behavior assays were performed as described previously (Tsuneto et al., 2020). For
360 feeding assay, three to five fifth instar larvae (Day 0) were put on individual Petri dishes, and the larval
361 mass before and after 1.5 h feeding was measured. An increase in larval mass was regarded as the
362 amount of food intake because no feces were observed after feeding. We adopted an increase in
363 body mass (%, w/w) as the index of food intake because a significant correlation between the amount
364 of food intake and the original body mass was observed via Pearson's correlation analysis (Fig. S4).
365 Mulberry leaves were collected around the campus of the Tokyo University of Agriculture and
366 Technology (Koganei, Tokyo, Japan) and stored at 4°C. To observe test bites, videos of silkworm
367 feeding on leaves were captured by a D5100 camera (Nikon, Tokyo, Japan) equipped with a telephoto
368 lens AF-S DX Micro Nikkor 85 mm (Nikon, Tokyo, Japan). The larvae were used 24–48 h after molting
369 to the fifth instar. To prevent nonspecific biting due to starvation, all larvae were fed on artificial diets
370 for 2 min before use.

371

372 **Tip recording**

373 Tip recording was performed as described previously (Tsuneto et al., 2020). In brief, the heads of
374 the fifth instar larvae (Day 0) were excised and used for further experiments within ~20 min. The
375 whole sensilla of MP were capped with a glass capillary (Erma Inc., Tokyo, Japan) filled with a
376 tastant solution dissolved in 5 mM NaCl using a micromanipulator (NARISHIGE, Tokyo, Japan). The
377 interval of stimulation was >1 min. When we observe desensitization in high concentration, we do
378 not include the data and test other larvae. We wash the silver wire to remove extraneous matter
379 especially after using high-concentrated solution. To confirm the silver wire is clean, we always test
380 response to 5 mM NaCl first before testing stimulants. We prepared taste solutions and their serial
381 dilution at time of use from powders (CGA and ISQ) and β-sitosterol stock solution (stored at -
382 20 °C). Electrical signals were amplified by a TastePROBE amplifier (Syntech, Hilversum, The
383 Netherlands), recorded via PowerLab 2/25 (AD Instruments, Sydney, Australia), and analyzed by
384 the LabChart software (AD Instruments). Spikes were counted from 0.1 to 1.1 s after the onset of
385 stimulation using custom codes written in MATLAB (Mathworks). Thresholds for counting spikes
386 were set from 0.3 to 1 mV depending on the baseline amplitude.

387

388 **Acknowledgments**

389 The authors thank Shingo Kikuta (Ibaraki University) and Masataka G. Suzuki (The University of
390 Tokyo) for technical assistance in calcium imaging at an early stage of this study and for establishing
391 the CRISPR-Cas9 system. This research was supported by the Japan Society for the Promotion of
392 Science (JSPS) KAKENHI (Grant Number 17K19261 for RS; 18J00733 for HE).

393

394 **Author contributions**

395 H.E., K.T., and R.S. designed the research; H.E. and K.T. performed calcium imaging and
396 electrophysiological recording studies; K.T. performed immunostaining and behavioral experiments;
397 H.E., T.Y., and D.M. generated knockout mutants under the supervision of K.I. and S.N. H.E. wrote
398 the manuscript with intellectual inputs from all authors.

399

400 **Conflict of interest**

401 The authors declare no conflicts of interest.

402

403 **References**

404 Asaoka. 2003. Ultrastructure of maxillary sensilla in the silkworm, Bombyx mori: differences among
405 strains? *J Insect Biotechnol Sericology*.

406 Briscoe AD, Macias-Muñoz A, Kozak KM, Walters JR, Yuan F, Jamie GA, Martin SH,
407 Dasmahapatra KK, Ferguson LC, Mallet J, Jacquin-Joly E, Jiggins CD. 2013. Female

behaviour drives expression and evolution of gustatory receptors in butterflies. *PLoS Genet* **9**:e1003620. doi:10.1371/journal.pgen.1003620

Chapman RF. 2003. Contact chemoreception in feeding by phytophagous insects. *Annu Rev Entomol* **48**:455–484. doi:10.1146/annurev.ento.48.091801.112629

Chapman RF, Bernays EA. 1989. Insect behavior at the leaf surface and learning as aspects of host plant selection. *Experientia* **45**:215–222. doi:10.1007/BF01951806

Cheng D, Mulder PPJ, van der Meijden E, Klinkhamer PGL, Vrieling K. 2017. The correlation between leaf-surface and leaf-tissue secondary metabolites: a case study with pyrrolizidine alkaloids in Jacobaea hybrid plants. *Metabolomics* **13**:47. doi:10.1007/s11306-017-1184-0

Chun MW. 1972. Dynamics of Feeding Responses in Pieris brassicae Linn. as a Function of Chemosensory Input: A Behavioural, Ultrastructural and Electrophysiological Study. Ann Arbor, United States: Wageningen University and Research.

Del Mármol J, Yedlin MA, Ruta V. 2021. The structural basis of odorant recognition in insect olfactory receptors. *Nature*. doi:10.1038/s41586-021-03794-8

Devitt BD, Smith JJB. 1985. ACTION OF MOUTHPARTS DURING FEEDING IN THE DARK-SIDED CUTWORM, EUXOA MESSORIA (LEPIDOPTERA: NOCTUIDAE). *Can Entomol* **117**:343–349. doi:10.4039/Ent117343-3

Engsontia P, Sangket U, Chotigeat W, Satasook C. 2014. Molecular evolution of the odorant and gustatory receptor genes in lepidopteran insects: implications for their adaptation and speciation. *J Mol Evol* **79**:21–39. doi:10.1007/s00239-014-9633-0

Fraenkel GS. 1959. The Raison d'Être of Secondary Plant Substances. *Science* **129**:1466–1470. doi:10.1126/science.129.3361.1466

Guo H, Cheng T, Chen Z, Jiang L, Guo Y, Liu J, Li S, Taniai K, Asaoka K, Kadono-Okuda K, Arunkumar KP, Wu J, Kishino H, Zhang H, Seth RK, Gopinathan KP, Montagné N, Jacquin-Joly E, Goldsmith MR, Xia Q, Mita K. 2017. Expression map of a complete set of gustatory receptor genes in chemosensory organs of Bombyx mori. *Insect Biochem Mol Biol* **82**:74–82. doi:10.1016/j.ibmb.2017.02.001

Heidel-Fischer HM, Vogel H. 2015. Molecular mechanisms of insect adaptation to plant secondary compounds. *Curr Opin Insect Sci* **8**:8–14. doi:10.1016/j.cois.2015.02.004

Jiao Y, Moon SJ, Wang X, Ren Q, Montell C. 2008. Gr64f is required in combination with other gustatory receptors for sugar detection in Drosophila. *Curr Biol* **18**:1797–1801. doi:10.1016/j.cub.2008.10.009

Kasubuchi M, Shii F, Tsuneto K, Yamagishi T, Adegawa S, Endo H, Sato R. 2018. Insect taste receptors relevant to host identification by recognition of secondary metabolite patterns of non-host plants. *Biochem Biophys Res Commun* **499**:901–906. doi:10.1016/j.bbrc.2018.04.014

Kikuta S, Endo H, Tomita N, Takada T, Morita C, Asaoka K, Sato R. 2016. Characterization of a ligand-gated cation channel based on an inositol receptor in the silkworm, Bombyx mori. *Insect Biochem Mol Biol* **74**:12–20. doi:10.1016/j.ibmb.2016.04.010

Letunic I, Bork P. 2021. Interactive Tree Of Life (iTOL) v5: an online tool for phylogenetic tree display and annotation. *Nucleic Acids Res* **49**:W293–W296. doi:10.1093/nar/gkab301

Liu X-L, Zhang J, Yan Q, Miao C-L, Han W-K, Hou W, Yang K, Hansson BS, Peng Y-C, Guo J-M, Xu H, Wang C-Z, Dong S-L, Knaden M. 2020. The Molecular Basis of Host Selection in a Crucifer-Specialized Moth. *Curr Biol* **30**:4476-4482.e5. doi:10.1016/j.cub.2020.08.047

Mang D, Shu M, Endo H, Yoshizawa Y, Nagata S, Kikuta S, Sato R. 2016. Expression of a sugar clade gustatory receptor, BmGr6, in the oral sensory organs, midgut, and central nervous system of larvae of the silkworm Bombyx mori. *Insect Biochem Mol Biol* **70**:85–98. doi:10.1016/j.ibmb.2015.12.008

Mang, Shu, Tanaka, Nagata, Takada. 2016. Expression of the fructose receptor BmGr9 and its involvement in the promotion of feeding, suggested by its co-expression with neuropeptide F1 in Bombyx …. *Insect Biochem*.

Naito Y, Hino K, Bono H, Ui-Tei K. 2015. CRISPRdirect: software for designing CRISPR/Cas guide RNA with reduced off-target sites. *Bioinformatics* **31**:1120–1123. doi:10.1093/bioinformatics/btu743

Ozaki K, Ryuda M, Yamada A, Utoguchi A, Ishimoto H, Calas D, Marion-Poll F, Tanimura T, Yoshikawa H. 2011. A gustatory receptor involved in host plant recognition for oviposition of a swallowtail butterfly. *Nat Commun* **2**:542. doi:10.1038/ncomms1548

Renwick JAA. 1989. Chemical ecology of oviposition in phytophagous insects. *Experientia* **45**:223–228. doi:10.1007/BF01951807

Renwick JAA, Lopez K. 1999. Experience-based food consumption by larvae of Pieris rapae : addiction to glucosinolates? *Entomol Exp Appl* **91**:51–58. doi:10.1046/j.1570-7458.1999.00465.x

Sato K, Tanaka K, Touhara K. 2011. Sugar-regulated cation channel formed by an insect gustatory receptor. *Proc Natl Acad Sci U S A* **108**:11680–11685. doi:10.1073/pnas.1019622108

Schindelin J, Arganda-Carreras I, Frise E, Kaynig V, Longair M, Pietzsch T, Preibisch S, Rueden C, Saalfeld S, Schmid B, Tinevez J-Y, White DJ, Hartenstein V, Eliceiri K, Tomancak P, Cardona A. 2012. Fiji: an open-source platform for biological-image analysis. *Nat Methods* **9**:676–682. doi:10.1038/nmeth.2019

Shii F, Mang D, Kasubuchi M, Tsuneto K, Toyama T, Endo H, Sasaki K, Sato R. 2021. Ultrasensitive detection by maxillary palp neurons allows non-host recognition without consumption of harmful allelochemicals. *J Insect Physiol* **132**:104263. doi:10.1016/j.jinsphys.2021.104263

480 Shim J, Lee Y, Jeong YT, Kim Y, Lee MG, Montell C, Moon SJ. 2015. The full repertoire of
481 Drosophila gustatory receptors for detecting an aversive compound. *Nat Commun* **6**:8867.
482 doi:10.1038/ncomms9867
483 Simon J-C, d'Alençon E, Guy E, Jacquin-Joly E, Jaquiéry J, Nouhaud P, Peccoud J, Sugio A, Streiff
484 R. 2015. Genomics of adaptation to host-plants in herbivorous insects. *Brief Funct Genomics*
485 **14**:413–423. doi:10.1093/bfgp/elv015
486 Singh S, Kaur I, Kariyat R. 2021. The Multifunctional Roles of Polyphenols in Plant-Herbivore
487 Interactions. *Int J Mol Sci* **22**. doi:10.3390/ijms22031442
488 Tsuneto K, Endo H, Shii F, Sasaki K, Nagata S, Sato R. 2020. Diet choice: The two-factor host
489 acceptance system of silkworm larvae. *PLoS Biol* **18**:e3000828.
490 doi:10.1371/journal.pbio.3000828
491 Vosshall LB, Amrein H, Morozov PS, Rzhetsky A, Axel R. 1999. A spatial map of olfactory receptor
492 expression in the Drosophila antenna. *Cell* **96**:725–736. doi:10.1016/s0092-8674(00)80582-
493 6
494 Wanner KW, Robertson HM. 2008. The gustatory receptor family in the silkworm moth Bombyx mori
495 is characterized by a large expansion of a single lineage of putative bitter receptors. *Insect*
496 *Mol Biol* **17**:621–629. doi:10.1111/j.1365-2583.2008.00836.x
497 War AR, Paulraj MG, Ahmad T, Buhroo AA, Hussain B, Ignacimuthu S, Sharma HC. 2012.
498 Mechanisms of plant defense against insect herbivores. *Plant Signal Behav* **7**:1306–1320.
499 doi:10.4161/psb.21663
500 Yang J, Guo H, Jiang N-J, Tang R, Li G-C, Huang L-Q, van Loon JJA, Wang C-Z. 2021.
501 Identification of a gustatory receptor tuned to sinigrin in the cabbage butterfly Pieris rapae.
502 *PLoS Genet* **17**:e1009527. doi:10.1371/journal.pgen.1009527
503 Yang K, Gong X-L, Li G-C, Huang L-Q, Ning C, Wang C-Z. 2020. A gustatory receptor tuned to the
504 steroid plant hormone brassinolide in Plutella xylostella (Lepidoptera: Plutellidae). *Elife* **9**.
505 doi:10.7554/eLife.64114
506
507

508

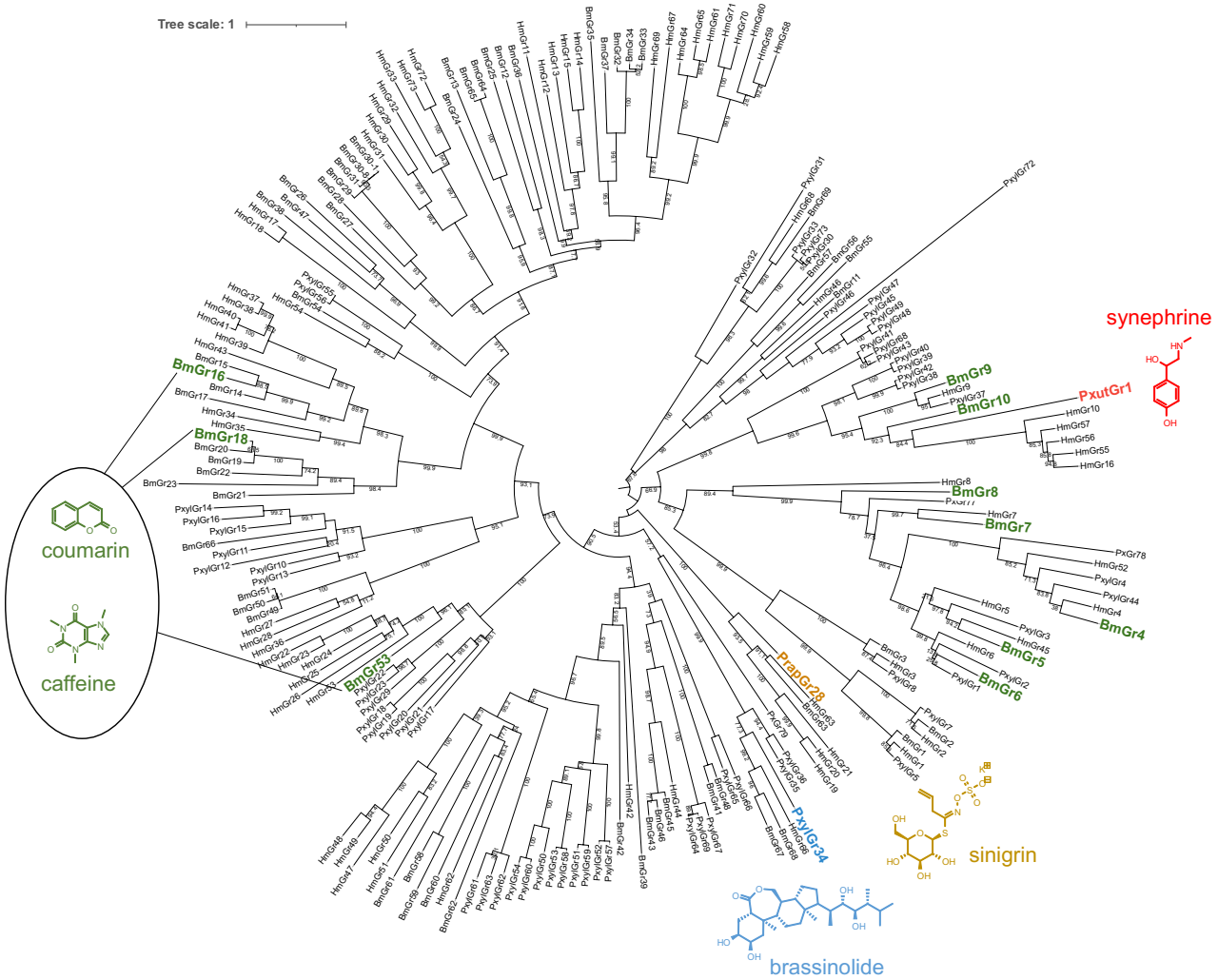

509

510 **Fig. 1. Phylogeny of the gustatory receptors in some lepidopteran insects.** The combination of
511 gustatory receptors and plant secondary metabolites as their ligands were highlighted with the same
512 colors as reported in previous studies [12,14,16,17]. Bm: *B. mori* (Guo et al., 2017); Pxyl: *P. xylostella*
513 (Engsontia et al., 2014); Hmel: *H. melpomene* (Briscoe et al., 2013).

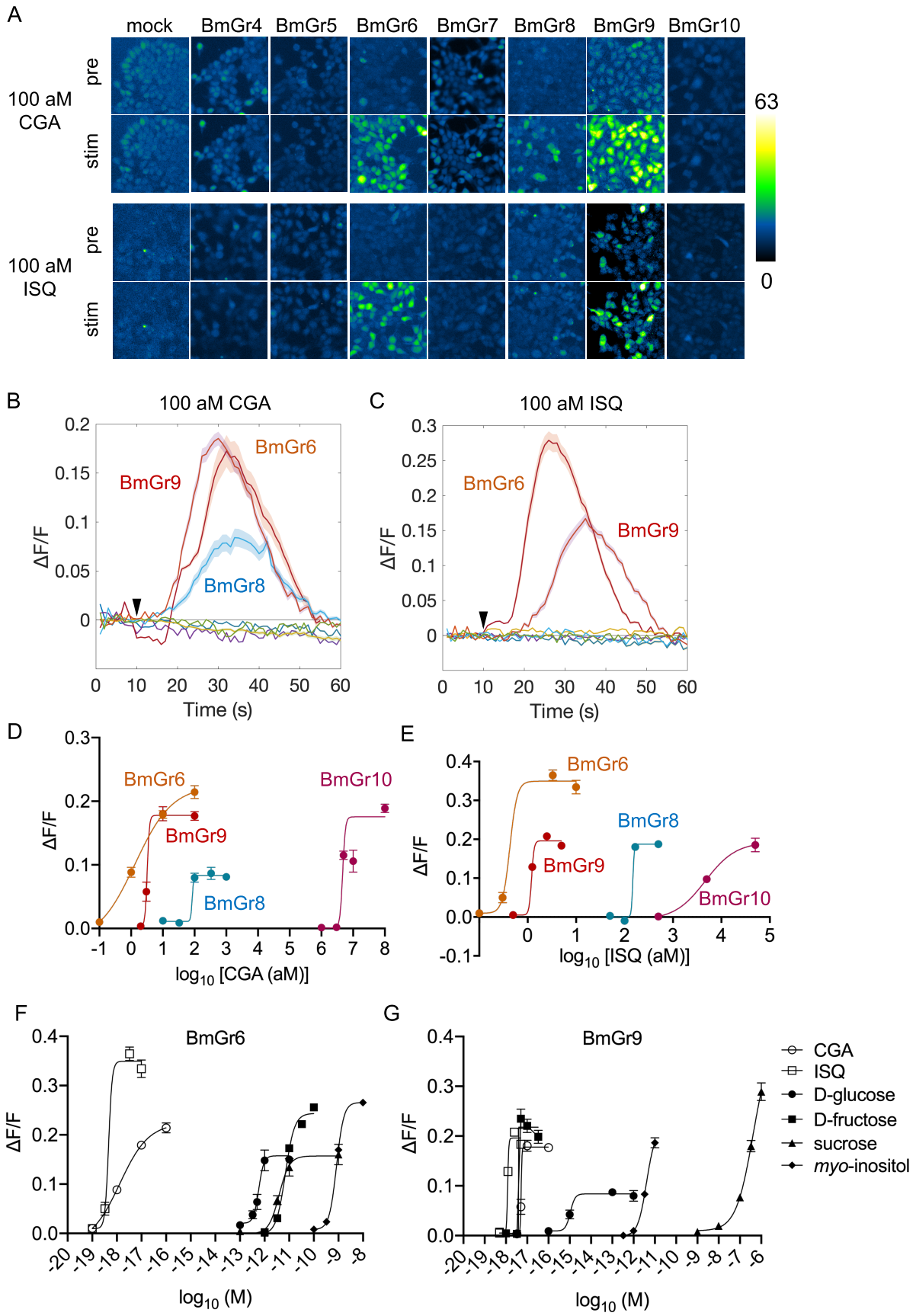
A
mock
BmGr4
BmGr5
BmGr6
BmGr7
BmGr8
BmGr9
BmGr10
100 aM CGA
pre
stim
100 aM ISQ
pre
stim
63
0
B
100 aM CGA
BmGr6
BmGr9
BmGr8
ΔF/F
Time (s)
C
100 aM ISQ
BmGr6
BmGr9
ΔF/F
Time (s)
D
BmGr6
BmGr9
BmGr8
BmGr10
ΔF/F
log10 [CGA (aM)]
E
BmGr6
BmGr8
BmGr9
BmGr10
ΔF/F
log10 [ISQ (aM)]
F
BmGr6
ΔF/F
log10 (M)
G
BmGr9
ΔF/F
log10 (M)
CGA
ISQ
D-glucose
D-fructose
sucrose
myo-inositol

515 **Fig. 2. Calcium imaging of BmGrs-expressing HEK293T cells.** (A) The response of BmGr-
516 expressing cells to 100 aM chlorogenic acid (CGA) and isoquercitrin (ISQ). The representative cell
517 images before (pre) and after (stim) stimulation. Fluorescent intensity is color-coded according to the
518 scale bar. (B and C) Time course of responses (ΔF/F) toward 100 aM CGA (B) and ISQ (C) (n = 30).
519 The arrowheads indicate the timing of the ligand application. (D and E) Dose-dependent responses
520 of BmGr6, BmGr8, BmGr9, and BmGr10 toward CGA (D) and ISQ (E). (F and G) Dose-dependent
521 responses of BmGr6 (F) and BmGr9 (G) toward CGA, ISQ, and sugars (B–G). Data are represented
522 as the mean ± SEM.

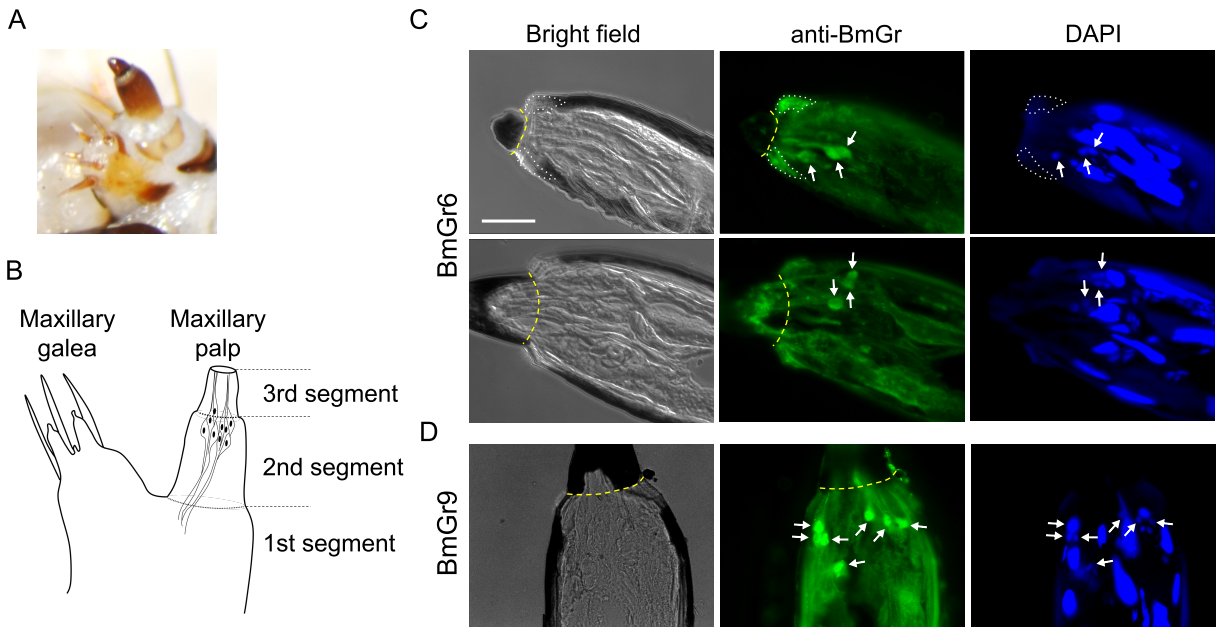

523

524

525 **Fig. 3. Immunostaining using maxillary palp (MP) BmGr6 and BmGr9 antibodies.** (A and B)
526 Image (A) and schematic diagram (B) of the maxilla of a silkworm larva. (C and D) Expression of
527 BmGr6 (C) and BmGr9 (D). Arrows indicate somas of immunoreactive sensory neurons. The areas
528 surrounded by broken white lines indicate the autofluorescence of the cuticle. Yellow broken lines
529 indicate the border between MP's second and third segments. Scale bar: 25 μm.

A

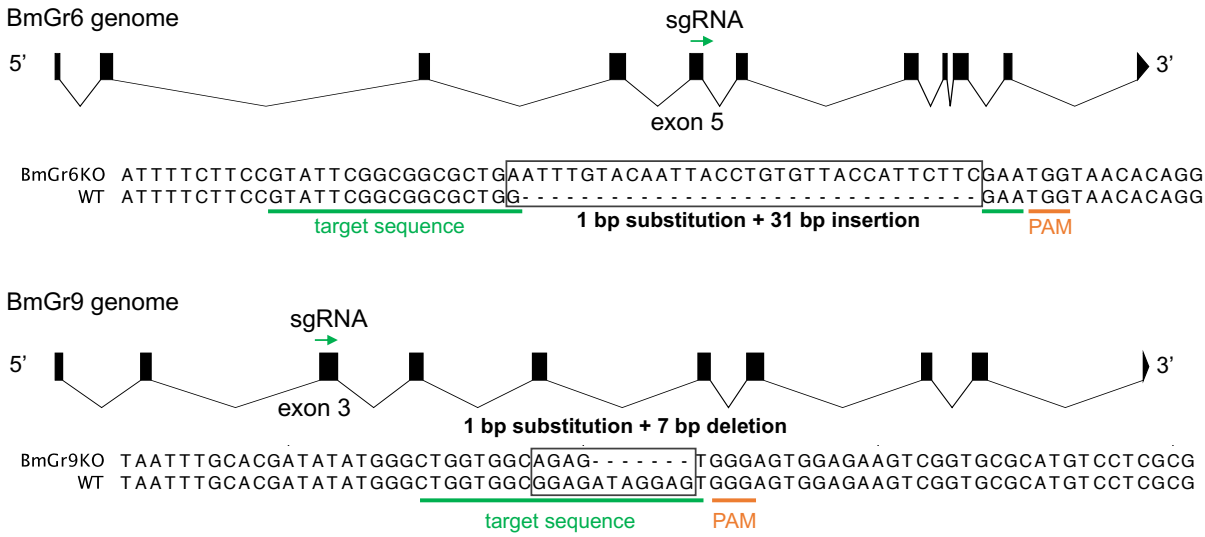
BmGr6 genome
sgRNA
5'
3'
exon 5
BmGr6KO ATTTTCTTCCGTATTCGGCGGCGCTGAATTTGTACAATTACCTGTGTTACCATTCTTCGAATGGTAACACAGG
WT ATTTTCTTCCGTATTCGGCGGCGCTGG- - - -

531 **Fig. 4. Generation and characterization of BmGr6-KO and BmGr9-KO larvae.** (A) Gene structures,
532 sgRNA target sites, including the adjacent protospacer motif (PAM), and obtained CRISPR/Cas9-
533 mediated mutations of *BmGr6* and *BmGr9*. Gene structures were drawn using Exon-Intron Graphic
534 Maker (http://wormweb.org/exonintron). (B) The body mass of freshly molted larvae (Day 0 of the fifth
535 instar) (n = 140–175). (C and D) The increase in larval body mass after 1.5 h feeding of artificial diets
536 (C) (n = 75–117) and mulberry leaves (D) (n = 60). (E) The proportion of larvae showing test biting
537 toward mulberry leaves. The biting of ten larvae was observed for one minute. Experiments were
538 repeated as independent biological replicates (n = 7–11). (F) Palpation time until the first bite toward
539 mulberry leaves (n = 23–99). Data are represented as the mean ± SEM. Statistical analysis was
540 performed by one-way ANOVA followed by the Tukey post hoc test. “ns” indicates no significant
541 difference; an asterisk indicates a significant difference (**$P < 0.01$; ****$P < 0.0001$).

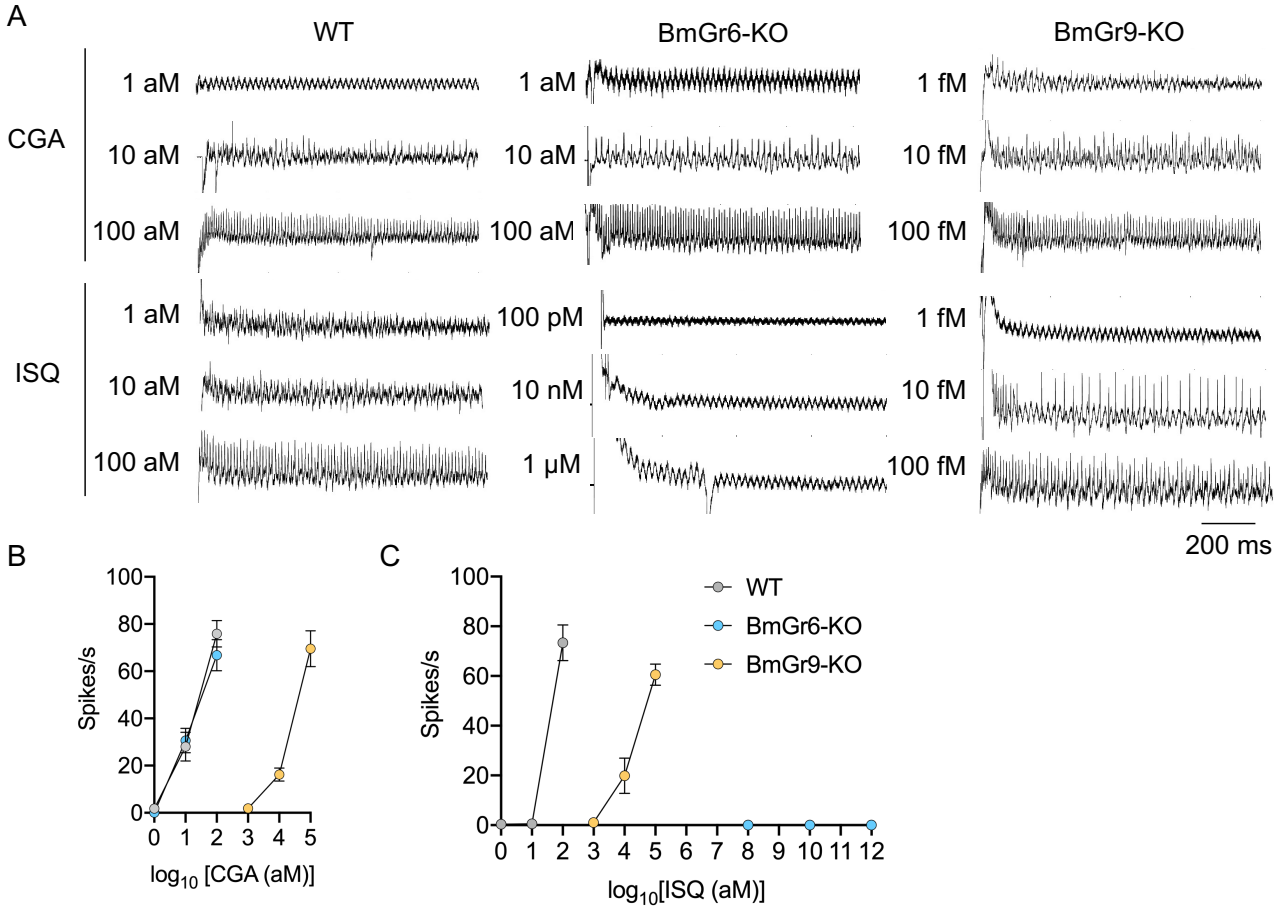

Fig. 5. Electrophysiological recordings of the maxillary palp (MP) in BmGr6-KO and BmGr9-KO larvae. The representative traces (A) and frequencies of action potentials from the whole MP sensilla in response to chlorogenic acid (CGA) (B) and isoquercitrin (ISQ) (C). Spikes were counted from 0.1 to 1.1 s after the onset of stimulation. Error bars are represented as SEM (n = 6–8).

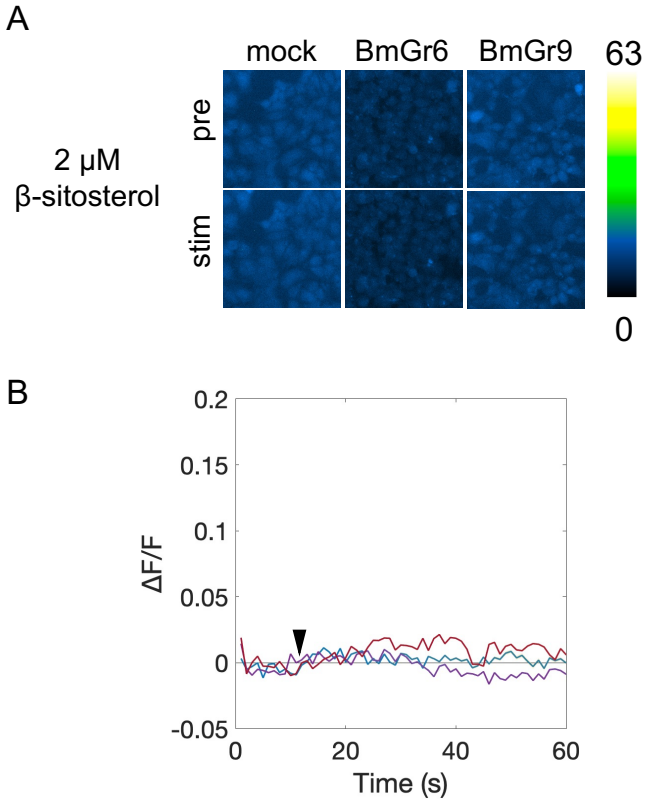

547

548 **Fig. S1. Response of BmGr6- and BmGr9-expressing cells toward β-sitosterol.** (A) The
549 representative cell images before (pre) and after (stim) stimulation by 2 μM β-sitosterol. Fluorescent
550 intensity is color-coded according to the scale bar. (B) Time course of responses (ΔF/F) toward 2 μM
551 β-sitosterol (n = 30). The arrowhead indicates the timing of the ligand application.

A

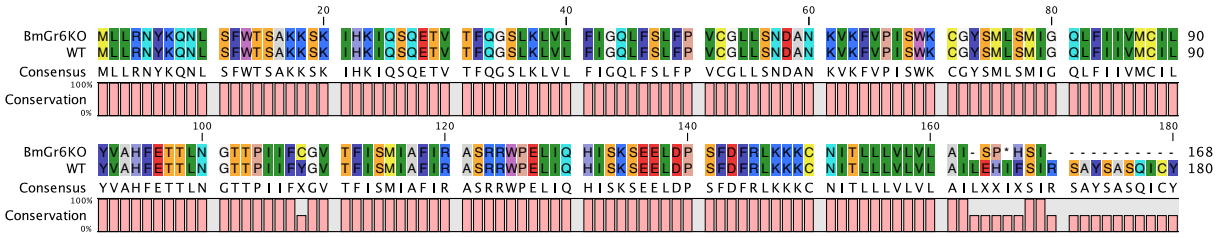

B

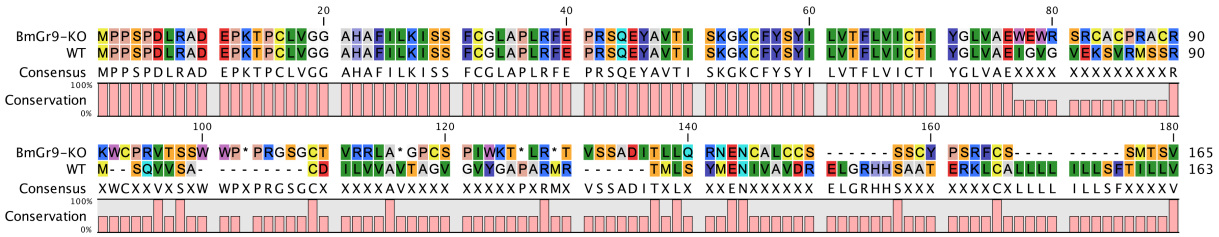

Fig. S2. Deduced amino acid sequences of truncated BmGr6 (A) and BmGr9 (B) in knockout larvae. The sequences were aligned using CLC Sequence Viewer 8 (CLC Bio, Aarhus, Denmark).

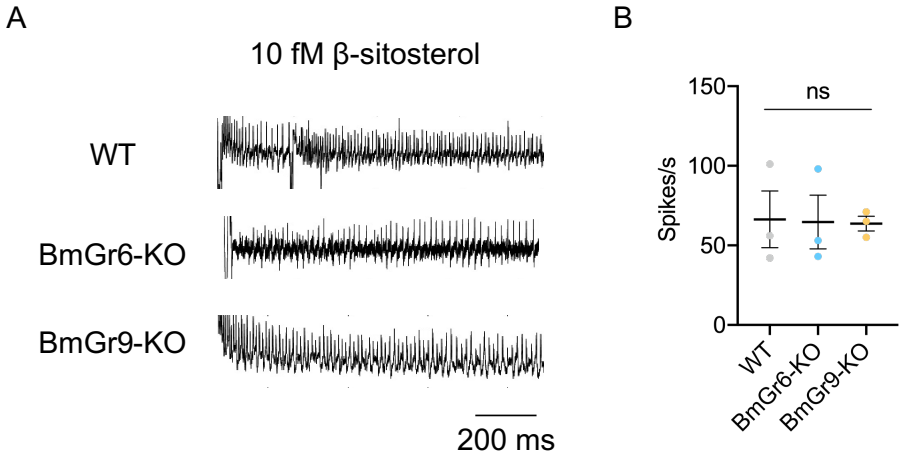

Fig. S3. Response of the maxillary palp (MP) in BmGr6-KO and BmGr9-KO larvae toward β-sitosterol. The representative traces (A) and frequencies of action potentials from the whole MP sensilla in response to 10 fM β-sitosterol (B). Spikes were counted from 0.1 to 1.1 s after the onset of stimulation. Data are represented as the mean ± SEM (n = 3). Statistical analysis was performed via one-way ANOVA followed by the Tukey post hoc test. “ns” indicates no significant difference.

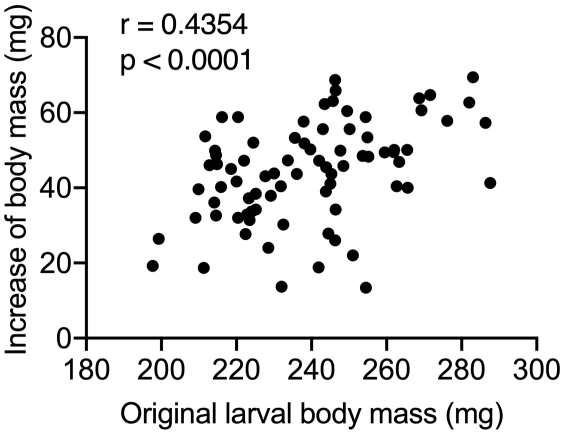

Fig. S4. Correlation between original body mass and feeding amount. Correlation coefficient (r) using Pearson correlation analysis (n = 80).

565 **Table S1. EC_{50} values of BmGrs in response to plant secondary metabolites (chlorogenic acid**
566 **(CGA) and isoquercitrin (ISQ)) and sugars.**
567

Gr	ligand	IC50 (aM)
BmGr6	CGA	1.329
BmGr8	CGA	~ 84.55
BmGr9	CGA	~ 3.226
BmGr10	CGA	4692479
BmGr6	ISQ	~ 0.4287
BmGr8	ISQ	~ 148.4
BmGr9	ISQ	~ 1.205
BmGr10	ISQ	4663

Gr	ligand	IC50 (M)
BmGr6	D-glucose	5.778E-13
BmGr6	D-fructose	6.993E-12
BmGr6	sucrose	3.909E-12
BmGr6	*myo*-inositol	8.378E-10
BmGr9	D-glucose	~ 1.059e-015
BmGr9	sucrose	4.198E-07
BmGr9	D-fructose	~ 3.903e-018
BmGr9	*myo*-inositol	4.051E-12

568